Since January 2020 Elsevier has created a COVID-19 resource centre with free information in English and Mandarin on the novel coronavirus COVID-19. The COVID-19 resource centre is hosted on Elsevier Connect, the company's public news and information website.

Applied Geography 143 (2022) 102702

Contents lists available at ScienceDirect

Applied Geography

journal homepage: www.elsevier.com/locate/apgeog

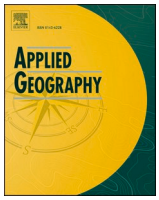

Risk assessment for precise intervention of COVID-19 epidemic based on available big data and spatio-temporal simulation method: Empirical evidence from different public places in Guangzhou, China

Shuli Zhou [a,b], Suhong Zhou [a,b,*], Zhong Zheng [c], Junwen Lu [a,b], Tie Song [d]

[a] School of Geography and Planning, Sun Yat-sen University, Guangzhou, 510275, China
[b] Guangdong Provincial Engineering Research Center for Public Security and Disaster, Guangzhou, 510275, China
[c] Center for Territorial Spatial Planning and Real Estate Studies, Beijing Normal University, Zhuhai, 519087, China
[d] Guangdong Provincial Center for Disease Control and Prevention, Guangzhou, 511430, China

ARTICLE INFO

Keywords:
COVID-19
Spatio-temporal spreading process
Big data
Gravity mode
Risk assessment
Precise intervention measures

ABSTRACT

Risk assessment of the intra-city spatio-temporal spreading of COVID-19 is important for providing location-based precise intervention measures, especially when the epidemic occurred in the densely populated and high mobile public places. The individual-based simulation has been proven to be an effective method for the risk assessment. However, the acquisition of individual-level mobility data is limited. This study used publicly available datasets to approximate dynamic intra-city travel flows by a spatio-temporal gravity model. On this basis, an individual-based epidemic model integrating agent-based model with the susceptible-exposed-infectious-removed (SEIR) model was proposed and the intra-city spatio-temporal spreading process of COVID-19 in eleven public places in Guangzhou China were explored. The results indicated that the accuracy of dynamic intra-city travel flows estimated by available big data and gravity model is acceptable. The spatio-temporal simulation method well presented the process of COVID-19 epidemic. Four kinds of spatial-temporal transmission patterns were identified and the pattern was highly dependent on the urban spatial structure and location. It indicated that location-based precise intervention measures should be implemented according to different regions. The approach of this research can be used by policy-makers to make rapid and accurate risk assessments and to implement intervention measures ahead of epidemic outbreaks.

1. Introduction

The spread of COVID-19 poses unprecedented challenges for governments throughout the world (Anderson et al., 2020). Strict non-pharmaceutical interventions have been adopted in many countries (e.g. China) to control the COVID-19 pandemic (Tian et al., 2020). China is gradually relaxing lock-down and social distancing measures when restarting economic and public activities. However, the prevention of COVID-19 in cities is still under large pressure and facing the disease resurgences before achieving herd immunity. This is because sporadic cases are continuously occurring, particularly in megacities with high-density populations. For example, a local outbreak occurred in Nanjing on 20 July 2021 had spread to more than twenty cities in the whole wave. It is urgent to implement location-based precise intervention measures to prevent resurgences of COVID-19 in cities, especially in the densely populated and high mobile public places. The measures emphasize the categorization and prioritization strategy according to the infection risk of different locations.

Citizens' daily activities and their interaction are one of reasons of the rapid spread of COVID-19 in cities. Residences, workplaces and public places are three important anchors of daily activities (Chai, 2013; Shen et al., 2015; Liu & Chai, 2015), which are also important nodes of disease transmission. Individuals at different places have different mixing patterns and contact intensity, causing different transmission risks. Previous researches have suggested that more than 80% of the contact occurred at home, workplaces, school, and public places (Mossong et al., 2008). Therefore, physical distancing interventions, such as stay-at-home, closure of school and workplaces, limiting the maximum number of people gathering, were conducted during the outbreaks of COVID-19 epidemic, as well as contact tracing on these daily activities

* Corresponding author. School of Geography and Planning, Sun Yat-sen University, Guangzhou, 510275, China.
E-mail address: eeszsh@mail.sysu.edu.cn (S. Zhou).

https://doi.org/10.1016/j.apgeog.2022.102702
Received 5 October 2021; Received in revised form 29 March 2022; Accepted 8 April 2022
Available online 20 April 2022

points. Individuals' daily contact includes close contact (regular encounters in household, and workplaces) and casual contact (random encounters at public places) (Kretzschmar et al., 2020; Yin et al., 2021). Close contacts have greater risk of transmission for person-to-person contact-transmissible infectious diseases such as COVID-19. It was reported that intra-family transmission made up 23% among local transmission (Chen et al., 2020). Besides, some infection cases happened at public places when people took entertainment activities such as dinner, playing cards and shopping (Chen et al., 2020; Wang et al., 2020). These public places, with dense population flow and confined spaces, would significantly contribute to the spread of the virus (Mossong et al., 2008). The outbreak of the epidemic at the early stage in China mainly happened at retail and recreation centers, such as Baodi Mall in Tianjin, Tuolong Mall in Harbin, and Yin-taishimao Mall in Wenzhou (Zhou et al., 2020a, 2020b). Since, the contacts (random encounters) in these places were difficult to track. It is more challenging to control the epidemic transmission occurring in public places than residences and workplaces. However, few studies assessed the disease transmission risk in public places, which is pivotal for reopening economic and public activities. Therefore, it is of great significance to discuss the location-based precise intervention measures of COVID-19 epidemic in public places.

Geographical big data, such as mobile phone data, social media data, GPS tracking data and other spatio-temporal big data, showed huge power in fighting against COVID-19 epidemic throughout the epidemiological cycle (Buckee et al., 2020; Budd et al., 2020; Zhou et al., 2020a, 2020b). Particularly, location-based mobile data made great contribution to public-health response to the global pandemic (Oliver et al., 2020). At the early-stage of the pandemic, location-based mobile data provided population and mobility information to help to understand COVID-19 transmission trends, identify potential transmission hotpots and trace contacts rapidly (Jia et al., 2020). During the middle-stage, location-based mobile data were used to build epidemiological model to predict the spread trend and estimate further infection risk (Lai et al., 2020; Wu et al., 2020). The dataset also helped to implement social distance measures, evaluate the effectiveness of different interventions on the progression of COVID-19 (Aleta et al., 2020; McKenzie & Adams, 2020; Wei et al., 2021; Yechezkel et al., 2020) and find the optimal measures of reopening economic and public activities at the late-stage (Yin et al., 2021; Huang et al., 2021). Location-based mobile data represented a critical tool for supporting public health decisions and actions of the government throughout the pandemic.

However, access to location-based mobile data is a challenge. Most mobile network operators, tended to be very reluctant to publish data to public and researchers (Oliver et al., 2020). Fine-scale or personal data (such as individual-level mobility data) were often inaccessible, due to legal and ethical considerations, as well as privacy and security concerns (Parker et al., 2020; Ienca & Vayena, 2020). Due to privacy consideration, people concerned that temporary emergency measures which monitor their movements may become pervasive and permanent (Budd et al., 2020; Calvo et al., 2020). Fortunately, some companies are gradually publishing subsets of aggregated data for research purposes during COVID-19 pandemic (China Data Lab, 2020; Hu et al., 2020). For example, daily aggregated origin-destination (OD) data from Baidu were used to evaluate the effect of travel restrictions and quarantine measures on COVID-19 transmission in China (Chinazzi et al., 2020; Kraemer et al., 2020). Google released weekly mobility reports in a sub-national scale (https://www.google.com/covid19/mobility/). Apple Inc. released a similar dataset of daily mobility (https://covid19.apple.com/mobility). However, these datasets cannot reflect intra-city mobility since they only represent travel flow between cities or provinces. Fortunately, public datasets, such as Tencent location request data (https://heat.qq.com) and Baidu Heat data (https://map.baidu.com/), are available with high spatial-temporal resolution (25 m*25 m) in the intra-city level. These datasets can be converted by mathematical methods to approximate the intra-city travel flows. The estimate of intra-city travel flows is incredibly valuable and essential for evaluating the disease transmission risk and develop precise intervention strategies of COVID-19 epidemic.

In summary, most of the previous research was limited in spatio-temporal transmission risk assessment at the micro scale (most of them at national, provincial, and regional level etc.), and the research results could not be directly adopted by the local government to implement precise intra-city intervention measures of COVID-19 epidemic. The micro level research plays an important role in providing the categorization and prioritization of intervention measures. Individual-based simulation has been proven to be an effective method for the risk assessment, but the acquisition of individual-level mobility data was limited. Moreover, the existing studies had little concern about the intra-city intervention measures, especially for the epidemic occurring in public places. Therefore, how to simulate the intra-city spatio-temporal spreading process with publicly available aggregated data under public health emergency events is an urgent task to be discussed.

In order to fill these gaps, this study used publicly available dataset to approximate dynamic intra-city travel flows by a spatio-temporal gravity model. It proposed an individual-based epidemic model and explored the intra-city spatio-temporal spreading process of COVID-19. After being calibrated and validated by the actual travel flows, the model simulated the spatio-temporal spreading process in different public places for developing location-based precise intervention measures. This study took the Guangzhou city (one of four megacities in China, with an area of about 7434 km^2 and nearly 20 million population) as a case, aiming to provide some universal insights for other megacities. The findings from this study would provide evidence-based guidelines for megacities. This study also provided a reliable method for other cities to respond to the public health emergency events based on their own situations.

2. Data and methods

This study used dynamic population distribution datasets to approximate intra-city travel flows through a spatio-temporal gravity model. It proposed an individual-based epidemic transmission model, which integrated the agent-based model and the susceptible-exposed-infectious-removed (SEIR) model, to simulate COVID-19 transmission dynamics and explore the spatio-temporal spreading pattern in different public places in Guangzhou.

2.1. Data sources

The dynamic population distribution dataset and the origin-destination (OD) flow dataset were used in this study. The dynamic population distribution dataset was used to quantify spatial interaction between grids as a proxy of mobility through gravity model. The second dataset was used as the validation of the first dataset.

The aggregated dynamic population distribution dataset: The dynamic population distribution dataset was provided by China Unicom Company, which had a market share of about 30%. The raw dataset contained one-day geocoding locations of nearly 7.05 million users of Guangzhou on 10-June-2020, a regular working day. A user's location was positioned by a signal tower when any communication behavior occurred such as calling, messaging, Internet search, or location updates. Even without any of these actions, the tower would detect the user's location by every 30–60 min. In the raw dataset, user' trajectories were made up of a series of locations. A *stay* was defined by the telecom company when a user stopped at the same location more than 0.5 h. The company has the original raw data of individual trajectories in the database, but it did not provide the raw data to researchers due to the privacy policy. Rather, the company aggregated users' locations to 500 m*500 m spatial grids from the database. It counted the number of users in each grid per hour. Finally 24-h dynamic distribution datasets were

provided to us. In particular, the users who stayed at the same grid for more than 20 h in one day were removed from the dataset, because they did not move all day and contributed little to the spread of disease.

The aggregated origin-destination flow dataset: The origin-destination flow (OD flow) dataset in the same day (10-June-2020) was also provided by the company. A *move* was defined by the spatial displacement of a user. Users moved from one stay to another stay. Movement between two stays was a *trip*. The start location of a trip defined an *origin (O)*, and the end location of a trip defined a *destination (D)*. Both O and D locations were geocoded by 500 m spatial grids. An OD flow was defined by the number of trips between the OD pair. Finally 24-h origin-destination flows between 500 m*500 m grids were provided to us.

Note that the population distribution dataset in each hour is not the instant population distribution at that moment, but the accumulated number of users within 1 h. Similarly, the OD flow in each hour is the accumulated number of OD trips within 1 h. The former dataset represents the number of people staying in each grid in each hour. It was used to estimate spatial interaction between grids as a proxy of mobility flows. The later dataset (actual OD flow) was used to validate the model. Specifically, we used a gravity model to estimate origin-destination mobility flow (estimated OD flow) based on dynamic population distribution datasets between two adjacent time periods (Section 2.2). The estimated OD flow was validated by actual OD flow data in section 3.1.

This study estimated OD flows from the dynamic population distribution data by a gravity model. We emphasized the use of estimated OD flows rather than actual OD flows. The reason was to make this study have wider applicability. Dynamic population distribution data with a high spatial-temporal resolution in the intra-city is publicly published and accessible, such as Tencent location-based big data and Baidu Heat data etc. In contrast, intra-city OD flow data is not easily accessible. In order to test the reliability of the model, this research used the dynamic population distribution data from mobile phone operator other than Tencent or Baidu, since the actual OD flow data for model validation were limited accessible from Tencent and Baidu. Our study aimed to use publicly available dynamic population data to simulate the spatio-temporal spreading process of COVID-19. It provided a novel approach to respond to the public health emergency events rapidly under limited access to individual-level or intra-city mobility data.

2.2. The gravity model

The gravity model is a useful spatial interaction modeling method, which has been widely applied in transportation and human geography research (Duffus et al., 1987). Many studies used it to measure commuting flow based on the spatial distribution of jobs-housing population (Zhang et al., 2017; Shi et al., 2020). However, the time dimension was rarely taken into consideration. This study adopted a production constrained gravity model to estimate the number of flows between origin-destination (OD) grids across different time periods.

$$G_{ij(t\to t+1)} = A_{i(t)} * O_{i(t)} * D_{j(t+1)} * f\left(d_{ij}\right) \tag{1}$$

$$A_{i(t)} = {}^{1}\Big/\sum_{j} D_{j(t+1)} * f\left(d_{ij}\right) \tag{2}$$

where $G_{ij(t\to t+1)}$ is the travel flow between the origin grid i and destination grid j from time t to $t+1$, $O_{i(t)}$ is the total number of people in the origin grid i at the time t, $D_{j(t+1)}$ is the total number of people in the destination grid j at the time $t+1$. $f(d_{ij})$ is a distance decay function, which usually follows a power law or an exponential distribution. $A_{i(t)}$ is a balancing factor which is constrained by destinations. The empirical evidence from Zheng et al. (2021) showed that $f(d_{ij})$ followed an exponential distribution in Guangzhou. The probability density function of an exponential distribution is given by:

$$f\left(d_{ij}\right) = \lambda e^{-\lambda d_{ij}} \tag{3}$$

$$\lambda = 1/\mathrm{E}\left(d_{ij}\right) \tag{4}$$

where λ is the decay parameter, which equals to the reciprocal of the expectation value of the exponential distribution. $\mathrm{E}(d_{ij})$ is the average travel distance between grids in this study. Previous studies showed that the average travel distance in Guangzhou was about 5 km (Lu et al., 2019). Hence, λ was set as 0.2 here. We used the above formula to calculate the spatial interaction value between grids across different periods and normalized it to 0–1 as the moving probability between two grids.

2.3. The epidemic model

We implemented an agent-based model integrated with the susceptible-exposed-infectious-removed (SEIR) model to simulate the dynamic spreading process of COVID-19. Agent is an autonomous computer entity. It is capable of interacting with other agents and adapting its behavior to the changing environment. Each agent has its own behavior according to specific rules which are given by researchers. Agents can represent any entities, e.g., people, animals or institutions etc.

In this model, agents represented people in the real world. Peoples' daily movements were assigned to the agents. The daily movements were determined by the spatio-temporal gravity model. Agent moved among grids in 24 h according to the result of the gravity model.

Based on the framework of SEIR, each agent has one out of four states: susceptible (S), exposed (E, not yet infectious), infectious (I), and removed (R, isolated, recovered, or otherwise no longer infectious, etc). The transmission was triggered by contacts between agents when agents were moving or stopping. Agents appearing in the same grid at the same time were regarded as contact. Specifically, once a susceptible agent (S) had contact with an infectious agent (I), the susceptible agent would be infected with a certain probability θ (the contact infection rate). If the susceptible agent was infected indeed, the state of susceptible agent would be transformed to "exposed" (E). At this stage the exposed agent could not infect other agents yet. After experiencing a 'latent period', the exposed agent would become 'infectious' (I) which could infect other agents. After lasting for an 'infectious period', the infectious agent would be isolated, recovered, or otherwise no longer infectious, and the state of the agent would change into "removed (R)". The removed agent was not infectious and could not be re-infected again. Related work of the model had previously been published (Zhou et al., 2021). Different from our previous model which needed individual-level mobility data, this model was improved to be applicable with aggregated data.

2.4. The epidemic model's parameterization and scenarios setting

The epidemic model involved three parameters: latent period, infectious period and the contact infection rate θ. According to our previous work (Zhou et al., 2021), each agent's latent period and infectious period followed the normal distributions with a mean of 3 days and a standard deviation of 1 day (latent period), and a mean of 8 days and a standard deviation of 2 days (infectious period) respectively. The parameter θ was estimated according to the basic reproductive number R_0. Studies from various sources have estimated different R_0 value from 2 to 7 (Li et al., 2020; Liu et al., 2020; Read et al., 2020; Sanche et al., 2020; Shen et al., 2020; Tang et al., 2020; Wu et al., 2020). This study set the value of R_0 as 4–5, a relatively medium value. The parameter θ was calibrated as 0.165. The calibration process was described in details in our previous work (Zhou et al., 2021).

Controlling epidemic transmission occurring in public places is a challenge for policy makers. How to implement intervention measures at such places is one of most concerned issues. Therefore this study

focused on disease transmission process originating in public places. Referring to a work which identified typical public places, commercial centers in Guangzhou (Chen et al., 2016), we selected eleven public places (Fig. 1). They were located in eleven different administrative districts of Guangzhou, representing the city center, inner-suburbs, and outer-suburbs locations respectively. We set eleven scenarios and simulated the epidemic spread process in these eleven public places respectively. We assumed that the epidemic started with several infectious agents and the rest agents were initially susceptible. Therefore, in each scenario, we randomly selected 10 agents located in the

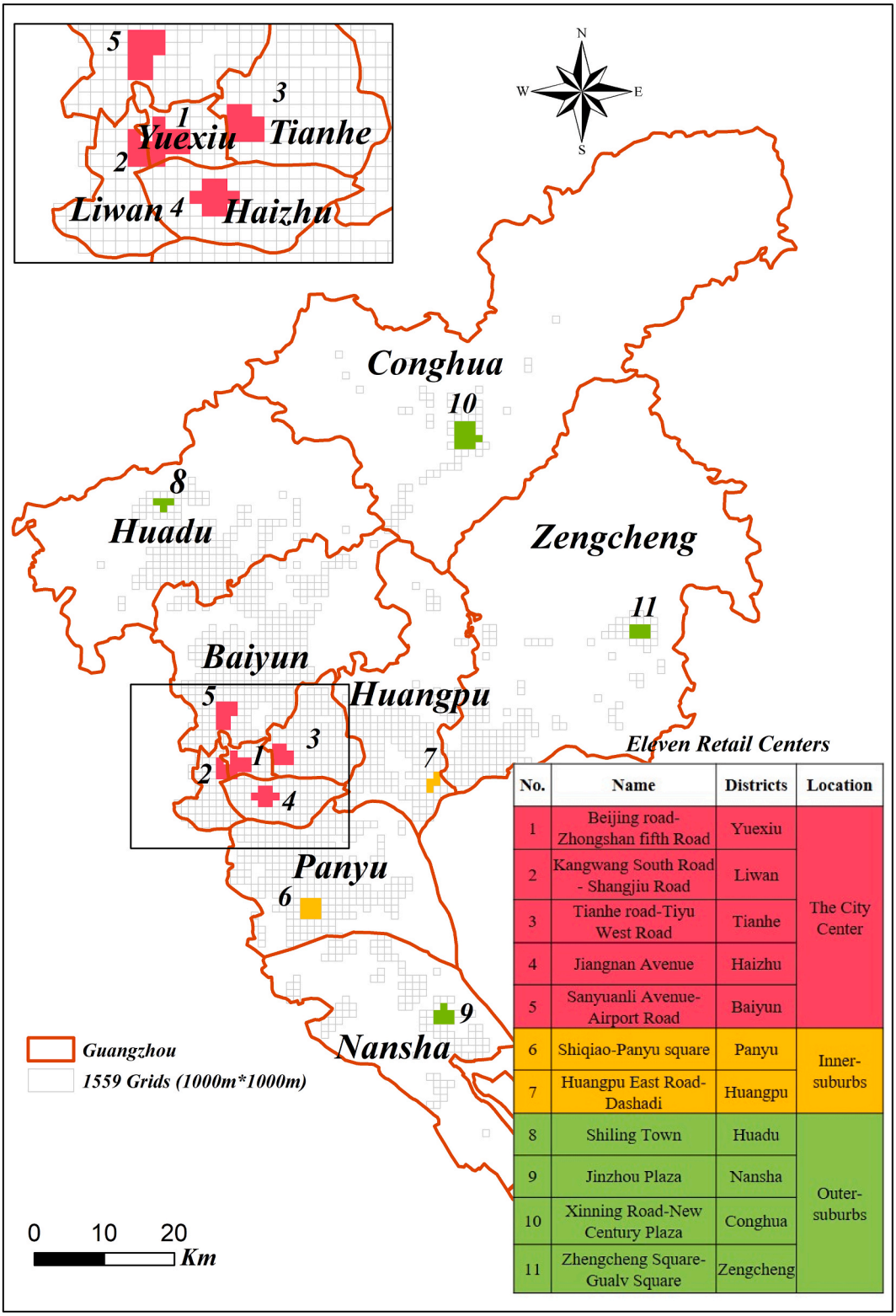

Eleven Retail Centers

No.	Name	Districts	Location
1	Beijing road-Zhongshan fifth Road	Yuexiu	The City Center
2	Kangwang South Road - Shangjiu Road	Liwan	
3	Tianhe road-Tiyu West Road	Tianhe	
4	Jiangnan Avenue	Haizhu	
5	Sanyuanli Avenue-Airport Road	Baiyun	
6	Shiqiao-Panyu square	Panyu	Inner-suburbs
7	Huangpu East Road-Dashadi	Huangpu	
8	Shiling Town	Huadu	Outer-suburbs
9	Jinzhou Plaza	Nansha	
10	Xinning Road-New Century Plaza	Conghua	
11	Zhengcheng Square-Gualv Square	Zengcheng	

Fig. 1. Study area and the location of eleven public places. Guangzhou was selected as a case study and it was divided 1000 m*1000 m grids. 1559 grids were finally selected as the study area and the population of these grids accounted for 91% of the total population of Guangzhou. We assumed that the epidemic occurred in eleven public places and it corresponded to eleven simulation scenarios (scenario 1–11).

corresponding public place as infective seeds. In scenario 1, we selected 10 agents located in the first public place as infective seeds. In scenario 2, we selected 10 agents located in the second public place as infective seeds. And so on. The other parameters (latent/infectious period/ θ) in the eleven scenarios were the same.

To improve the efficiency of the simulation, we only chose the population distribution data at four periods (6:00, 12:00, 18:00, and 24:00) which represented the greatest differences of population distribution in one day. These four periods' data was a reflection of daily activity, such as early at home, workplaces at noon, shopping or leisure in public places, and back home at night. Although some people will leave workplaces at noon, a study from Guangzhou showed that 87.5% of people would have lunch or take a rest at or near their workplaces (Zhou & Deng, 2010). 18:00–19:00 was a small peak period for eating out and taking leisure activities (Song et al., 2017). Therefore, based on four periods' population distribution data, we used the gravity model to estimate OD flows between 6:00 and 12:00 (estODflow_0612), between 12:00 and 18:00 (estODflow_1218), and between 18:00 and 24:00 (estODflow_1824). The estimated OD flows were then normalized to 0–1 as the movement probability among grids at different time periods.

The simulation process is as follows. First, we generated 100,000 agents in proportion to the spatial distribution of the population at 6:00 in the morning in Guangzhou. Second, we set each agent's latent/infectious period and the contact infect rate according to the above parameterization. And we randomly select 10 agents located in the corresponding public places in each scenario as infectious agents and the rest agents were initially susceptible. Third, the 100,000 agents started their daily movements among OD grids from 6:00 to 24:00 according to the normalized probability matrix which was previously estimated from the gravity model. The matrix showed the moving probability by which an agent travelled from one grid to another gird. For example, the agent at 6:00 would make decisions whether to move or not from 6:00 to 12:00, according to normalized estODflow_0612. Then it would continue to move or not according to normalized estODflow_1218 until the end of the day (24:00). In the next day, the agent would continue the movement similarly. Fourth, after finishing each movement, the simulation system would judge whether the agent would be infected or not, and whether its state would change or not. Once being infected, the state of the susceptible agent would become "exposed". After experiencing a 'latent period', the state would turn into "infectious", and after an 'infectious period', the state would become "removed". Finally, the simulation stopped when there was only susceptible and removed agents in the model.

The model would output the attack rate (the proportion of agents who have been infected), durations (the lasting days), the number of new exposed agents per day (daily-newE), the number of new infected agents per day (daily-newI), the number of new removed agents per day (daily-newR), and the spatial distribution of susceptible/exposed/infected/removed agents per day. For each scenario, we simulated 50 times to balance the stochastic effect.

Besides, as the urban built-up area only accounts for 17.5% of the total area of Guangzhou, we only selected the top 20% grids to represent the built-up area according to the population distribution. Further, in order to improve the simulation efficiency and evaluate the spatio-temporal transmission risk rapidly, we aggregated the 500 m*500 m spatial grids into 1000 m*1000 m grids. The distance between two parallel main roads in China is 700–1200 m. 1000 m-grid is a suitable and commonly used spatial scale (Chen et al., 2016). Finally, 1559 grids were selected as the study area (Fig. 1), and the population of these grids accounted for 91% of the total population of Guangzhou.

3. Results

The OD flow estimated by the gravity model (hereinafter estimated OD flow) was firstly validated by comparing with actual OD flow. Then the natural transmission process occurring in eleven public places were simulated respectively, based on the estimated OD flow. Finally, the evolutionary process of the epidemic was analyzed from the perspectives of time and space.

3.1. Validation of the gravity model

To evaluate the accuracy of estimated OD flow, we validated it with actual OD flow by comparing the number of trips from a grid unit to other grids. As mentioned above, we estimated three groups of OD flows: 6:00–12:00 (estODflow_0612), 12:00–18:00 (estODflow_1218), and 18:00–24:00 (estODflow_1824). Meanwhile, we calculated the actual OD flows between 6:00 and 12:00 (actODflow_0612) from the aggregated origin-destination flow dataset, which was the sum of actual OD flow at 6:00, 7:00, 8:00, 9:00, 10:00, 11:00 and 12:00. ActODflow_1218 and actODflow1824 were similarly calculated. Estimated OD flows and actual OD flows were displayed in a 1559*1559 matrix. For each O grid, it has had a set of outgoing flows to other D grids. The set of estimated outgoing flows and the actual outgoing flows from the same O grid can be compared. Then each O grid had an R square value of estimated and actual outgoing flows. The spatial distribution of R square of each O grid was shown in Fig. 2. The mean value of R square value between estODflow_0612 and actODflow_0612 was 0.72. The average R square value at the other two time periods were 0.73 (Figs. 2b) and 0.74 (Fig. 2c) respectively. They also showed similar spatial distributions. The result indicated that it was acceptable to use the dynamic population data at different periods by the gravity model to estimate travel flows.

3.2. Temporal process of the epidemic transmission

Table 1 showed the simulated attack rate and durations in eleven scenarios, under natural transmission without any intervention. The final attack rate is the proportion of agents who have been infected at the end of an epidemic. The duration is the time length between the start and the end of an epidemic. For each scenario, we simulated 50 times to balance the stochastic effect. The results suggested that the attack rate increased with the distance from city center, except for two public places in the furthest outer-suburbs (scenario 10 and 11).

The dynamic process of attack rate with time in each scenario was shown in Fig. 3, as well as daily-newE/daily-newI/daily-newR (the number of new exposed/infected/removed agents per day). The attack rate (Fig. 3a) increases rapidly, then reaches a peak and gradually flattens, presenting an S-shape curve. While, the other three curves (Fig. 3b–d) show inverted U-shaped shapes, increasing firstly and decreasing afterward. Eleven scenarios could be classified into four levels based on the temporal changes.

Scenario1-5 (public places in the city center) showed the highly similar time trend and could be classified as the first category. They were the earliest to spread among all the scenarios. The attack rate (Fig. 3a) increased explosively from the 10th day and became stable after the 20th day. The daily-newE increased sharply from the 7th day, reached the peak on the 14th day and then began to decline, down to zero after the 22nd day (Fig. 3b). The daily-newI began to increase three day later than daily-newE, and took about one week to reach a turning point on the 18th day (Fig. 3c). Because, the infected cases would be removed through an 'infectious period', the daily-newR followed the same trend curve with "daily-newI" after a few days later.

Scenario 10 and scenario 11 (public places in the rural outer suburbs) belonged to the same category. The attack rate of the two scenarios, less than 2%, was the lowest in the all scenarios. They were located farthest from the city center. The epidemic occurring in this places didn't spread widely and the transmission stopped after local spread within a small area.

Scenario 8 and scenario 9 (public places also located in the outer suburbs) could be classified into another category. The final attack rates of these two scenarios were the highest (82% and 80%) among all the

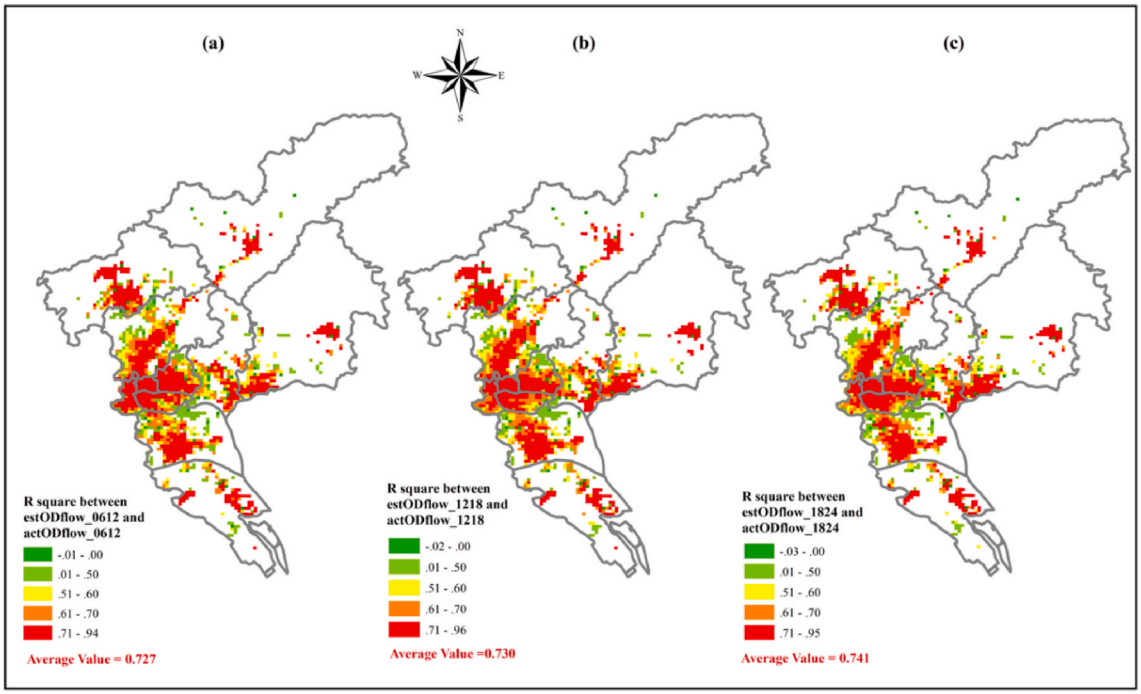

Fig. 2. The spatial distribution of R square of each gird between estimated OD flow by gravity model and actual OD flow. The outgoing flows from a same O grid were compared at from 6:00 to 12:00(2a), from 12:00 to 18:00(2b), and from 18:00 to 24:00(2c).

Table 1
The final attack rate under eleven scenarios.

Location of public places	Scenarios	Attack rate (%,Median [1st,3rd])	Durations (Days, Median[1st,3rd])
The City center	Scenario1	77.31 [77.21,81.30]	118 [113,124]
	Scenario2	77.36 [77.19,81.08]	128 [116,143]
	Scenario3	77.37 [77.18,81.37]	113 [104,122]
	Scenario4	77.34 [77.21,81.34]	115 [113,126]
	Scenario5	77.32 [77.22,77.43]	119 [101,131]
Inner suburbs	Scenario6	77.57 [77.37,80.41]	130 [112,137]
	Scenario7	77.83 [77.78,78.05]	132 [115,138]
Outer suburbs	Scenario8	82.07 [82.01,82.09]	117 [112,125]
	Scenario9	80.20 [80.01,80.43]	140 [126,162]
	Scenario10	1.71 [1.70,1.71]	43 [42,49]
	Scenario11	1.46 [1.45,1.46]	38 [36,38]

scenarios. Simultaneously, they had the slowest speed and the longest transmission duration. The attack rate increased explosively from the 20th day, which was 10 days later than the first category (Scenario 1–5). The daily new infected cases reached the peak at the 25th day, with the same lag time of ten days compared with Category I.

The remaining scenario 6 and scenario 7 could be summarized into the last category. The final attack rate of these two scenarios was more than 77.5%, fluctuating between Category I (scenario 1–5) and Category III (scenario 8–9). The peaks of the number of daily new E/I/R cases were 2–3 days later than Category I, but 6–8 days earlier than Category III. The two areas were close to the periphery of the city center, but located in the inner side of suburbs.

The above results indicated that the transmission time varied across the location, and the closer the distance from the urban center was, the earlier the transmission started. This time trend is important because it demonstrated different time windows for the government to deal with the epidemic and let policy makers to know which areas need to be prioritized in the fight against COVID-19.

3.3. Spatial process of the epidemic transmission

The spatial spreading process of COVID-19 in scenario 1–11 was shown in Fig. 4. Similar with the classification of time trends, the spatial patterns demonstrated the same classification. Scenario 1–5 exhibited a hierarchical spatial pattern of “one core and three vertices”. Scenario 6–7 presented a pattern of “one sword with two wings”. Scenario 8–9 showed a “Northwest-Southeast” corridor distribution and a skew T-shaped distribution finally. While scenario 10–11 did not spread widely, but stopped after only local propagation in a small area nearby.

The spatial spreading process of COVID-19 and its evolution characteristics in scenario 1 were shown in Fig. 4a. The spatial evolution of scenario 2–5 showed a high degree of agreement with scenario 1 and were not shown due to space limitation. The spatial distribution of the attack rate every 20 percentage point’s increment were presented. The spatial transmission was characterized by the process from core cluster outbreak in the central five districts at the early stage to comprehensive dispersion occurrence at the late stage, from the central to the South, then to the East and finally to Northwest. The spatial distribution exhibited a hierarchical pattern of “one core and three vertices”. The one core was the central five districts: Yuexiu, Liwan, Tianhe, Haizhu and Baiyun districts. The three vertices were Panyu district, Huangpu-Luogang junction, and Huadu district respectively. The core five districts were the earliest to spread the epidemic, as well as the most serious, and the three axes appeared gradually in sequence.

Fig. 4b showed the spatial spreading process from scenario 6. When Covid-19 broke out in Shiqiao-Panyu Square, the epidemic first appeared sporadically in Panyu district, and spread to the central five districts simatenously; then gradually spread to Huangpu district in the eastern suburbs and further to the periphery (Huangpu-Zengcheng junctions); finally migrated to Huadu district in the outer suburbs. The spatial distribution presented a pattern of “one sword with two wings”. In other words, Panyu as well as central five districts was the body of the arrow, Huangpu-Luogang junction and Huadu were the two wings respectively. A very similar spatial pattern was seen in scenario 7 (Fig. 4c), when sporadic cases occurred in the suburb of Huangpu district. The vertical arrow turns into a horizontal arrow, with Huangpu

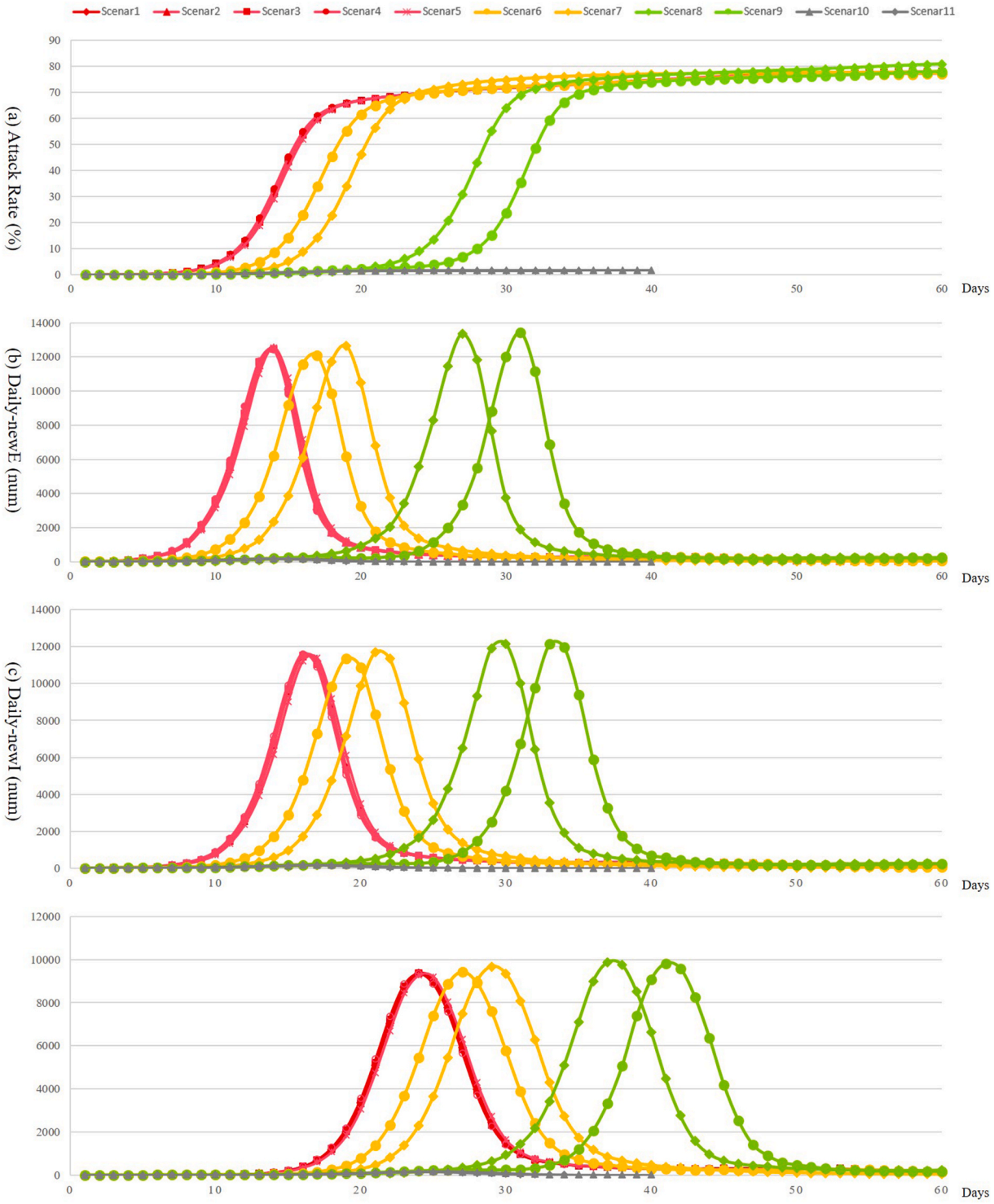

Fig. 3. The temporal process of output results in Scenario 1–11. Attack rate(3a, the proportion of agents who have been infected); The number of new exposed agents per day(3b); the number of new infected agents per day(3c); The number of new removed agents per day(3d). The horizontal axis represents from the 1st day to the 60th day.

and the central five districts as the body, and Panyu as the left shoulder, while Huadu as the right shoulder.

When the epidemic occurred in the outer suburbs (scenario 8–9), it showed completely different spatial patterns (Fig. 4d–e). The epidemic first spread locally in nearby areas until the nearby areas was almost completely occupied. After that, the step of transmission gradually approached to the central area. Once the torch fire reached to the central area, it would be a large-scale outbreak in the urban five districts. Meanwhile, the confirmed cases showed a "Northwest-Southeast" corridor distribution. Then, the corridor changed its direction and extended eastward, from the inner suburbs (Huangpu district) to the outer suburbs (Zengcheng district). At last, the spatial distribution presented a skew T-shaped distribution.

Finally, we found that the epidemic occurring in the rural outer suburbs (scenario 10–11) did not spread widely, but stopped after only local propagation in a small area nearby (Fig. 4f). Interestingly, we

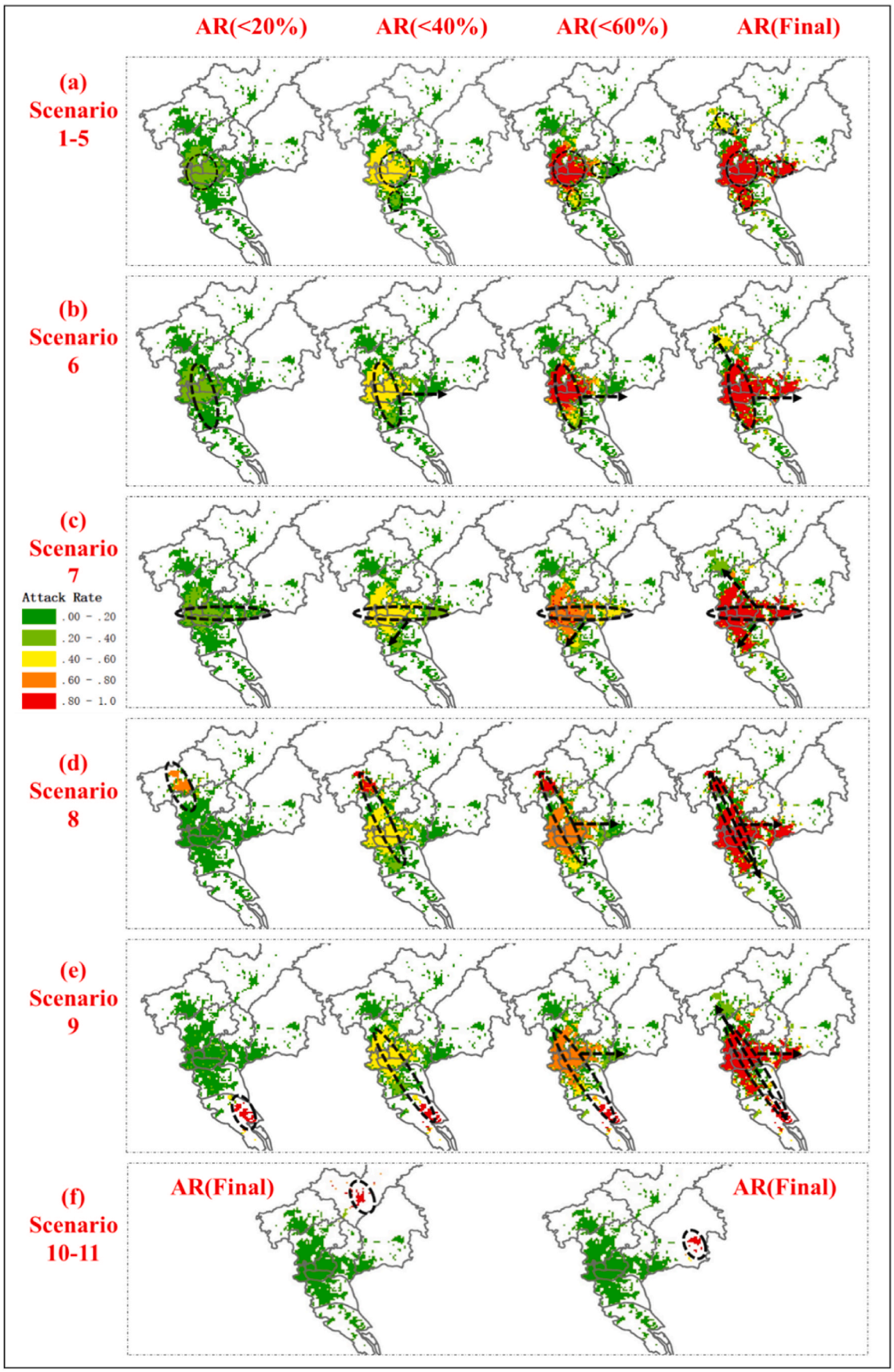

Fig. 4. The spatial spreading process under scenario 1–11. AR means attack rate (the proportion of agents experiencing infection).

noted that the epidemic occurring in these two areas seldom spread to other regions, nor did other regions to these two areas.

4. Summary

Integrating the time and space dimensions, the epidemic transmission pattern in eleven public places could be summarized into four categories: scenario 1–5 (the city center), scenario 6–7 (inner suburbs), scenario 8–9 (outer suburbs), and scenario 10–11 (satellite towns). The differences of epidemic transmission pattern in different location were associated with the distance to the city center.

5. Discussion

This study used publicly available datasets to approximate dynamic intra-city travel flows by a spatio-temporal gravity model. It proposed an individual-based epidemic model and explored the intra-city spatio-temporal spreading process of COVID-19 in different public places. The analysis could support the location-based precise intervention measures for policymakers and provide guidance for public health emergency events in the future.

By comparing the epidemic spread process in eleven public places, we identified four spatial-temporal patterns of COVID-19 transmission process in Guangzhou. We discovered that some areas had higher probability of being affected by COVID-19 than others. The transmission pattern was highly dependent on the urban spatial structure and location. Hence, location-based precise intervention measures should be implemented according to various epidemic transmission modes in different regions.

Our simulation results demonstrated that the transmission of the epidemic was the fastest and the epidemic peak happened the earliest when it occurred in the central area. The epidemic will spread over the core five districts in a short time, exerting great pressure on health-care system. Since the central area has the highest population density and the heaviest travel flows, the government should vigorously pursue strong physical distancing interventions on the central five districts to avoid the explosive growth of the epidemic, for example, stay-at-home, schools and workplaces closures, cancellation of public events, and movement restrictions (Dlamini et al., 2020; Huang et al., 2021). Meanwhile, intense screening and testing, and contact tracing efforts should also be reinforced in such areas (Yin et al., 2021). In addition, mask wearing and health elimination in public places, especially in the densely populated facilities (such as stations, supermarkets, restaurants, and shopping malls, etc.) should be highly promoted. Besides, our simulation results also suggested that the epidemic sourcing from urban center seldom reached the outer suburbs, especially satellite cities. Implementing strong physical distancing measures in these areas can be mismatched. The government could encourage residents of these areas to take protective measures and health monitoring, exercise moderately and improve their own immunity.

The epidemic outbreak in inner suburbs with medium population density was approximately 2–3 days later than central areas. But, the epidemic would spread rapidly to the central five districts at the same time of transmission nearby. Since the main function of recreational business district is to offer recreation, entertainment and shopping for local residents and residents living in the peripheral areas, and the activities of residents living nearby promoted the epidemic spread. Shiqiao-Panyu Square in Panyu (scenario 6) and Dashadi in Huangpu (scenario 7), as the sub-centers of Guangzhou, were initially built to evacuate the population in the central area, reduce the housing pressure in the center and provide suitable housing and employment for the rapidly growing urban population (Jiang et al., 2012). Many people living here commuted to central areas as well as working nearby, causing the suburbs and the five center districts being affected at the same time. Although the governments had 2-3 more days to deal with it, the urgency and severity of the epidemic is no better than the central areas. Therefore, close contacts tracing would be the most important control measure in these places. Moreover, in order to avoid a large-scale outbreak of the epidemic, social distancing measure of limiting contact and restricting traveling in and out of such places should be implemented as early as possible. Mask wearing and disinfection in populated areas would still be required to lower the infection rate. Extensive temperature check at public places to identify people with fever and limit their out-of-home activities would also be very important.

The third spatial-temporal pattern occurred in outer suburbs and had the lowest transmission speed but the highest attack rate. With the increasing distance from the central area, the residents' long-distance commuting demand gradually decreased (Zhou & &Yan, 2005). For a long time, the epidemic only spread in the community, which gave the government a big time-window to respond to the epidemic. Hence, controlling the spread of the epidemic sourcing from these areas as early as possible would be essential. The government should take a fast emergency response to ensure that there are no outflows from such areas. Prevention of community transmission is among the most urgent issues for these areas. Once the epidemic spreaded to urban area, it would evolve a city-wide emergency event which brings huge burden for the existing healthcare system and requires huge amounts of resources to prevent. Since the total number of infected people would be much larger than the total number infections caused by the epidemic occurring in the urban center or the inner suburbs. In other words, the epidemic sourcing from the outer suburbs would spread to not only the local community but also to the urban center, while the epidemic from the urban center was less likely to reach the outer suburbs. Therefore the government should spare no efforts to avoid onward transmission to urban areas. The epidemic control in Xiaoguozhuang Village, Shijiazhuang City, Hebei Province, China was a very successful example based on this situation (Chinanews, 2021).

Differently, satellite towns with low population density can control the transmission without implementing strong physical distancing measures. Zengcheng and Conghua, known as the back garden of Guangzhou, have become important satellite towns to receive the population spillover from the urban center. They provide comfortable living condition, sufficient local employment opportunities and sound infrastructure to attract people to settle down. They are relatively isolated to the city and most residents have their daily activities within a local range. Hence, physical distancing measures can be implemented locally at the satellite city, and the other parts of the city conduct social and economic activities normally.

Besides, we only selected four typical periods' population distribution data among 24-h daily activities. The intent is to provide a method to make rapid spatio-temporal risk assessment respond to public health emergency under the limited computing ability. There is no doubt that the simulation with high temporal resolution will certainly have more accurate results. Of course, our model also supports high spatio-temporal resolution aggregated datasets.

Several limitations should be mentioned. First, our aggregated data only include one weekday. Activities in the weekend also contribute to the epidemic, but we did not specify the transmission pattern in the model simulation. Second, individual socio-demographic attributes, such as age-specific susceptibility to COVID-19 infection were not included in our model. Third, we assumed that the removed person will be permanently immunized. However, there is a probability that infected people could be infected again. We do not consider this situation in our current work. We will develop a model which simulates the re-infectious characteristics of the COVID-19 in the future.

6. Conclusions

This study used publicly available datasets to predict intra-city epidemic transmission process in different public places. The results indicated that the accuracy of dynamic intra-city travel flows estimated

by available big data and gravity model is acceptable. The spatio-temporal simulation method well presented the process of COVID-19 epidemic. It suggested that location-based intervention measures of COVID-19 epidemic should be implemented according to different epidemic transmission modes, which was crucial for other megacities around the world. The work also identified different time windows for the government to deal with the epidemic. This is important for government to know which areas need to be prioritized with preparedness and response measures in the city. The approach of this research can be adopted by policy-makers in other countries to make rapid and accurate risk assessments and to implement intervention measures ahead of ongoing outbreaks.

Author contributions

S.L.Z and S.H.Z. designed the experiments. S.L.Z. analyzed data, created the models and ran the simulations. S.L.Z., Z.Z. and S.H.Z. interpreted the results. S.L.Z. wrote the Article. Z.Z. J.W.L. and T.S. edited and revised the Article.

Statement

The following are our statements for the submitting of our paper entitle "Risk assessment for precise intervention of COVID-19 epidemic based on available big data and spatio-temporal simulation method: Empirical evidence from different public places in Guangzhou, China" to *Applied Geography*:

(1) The manuscript is our original research;

(2) It has not been submitted elsewhere in print or electronic form to another journal or as a proposed book chapter;

(3) It has not been published previously or otherwise accessible to the public (e.g., posted on website);

(4) No similar or exact submission will be sent elsewhere until your review is completed.

(5) Funding Statement: This research has been supported by the Key-Area Research and Development Program of Guangdong Province, China (2020B0202010002), National Natural Science Foundation of China (71961137003 and 41871148), Philosophy and Social Science Planning Project of Guangdong Province, China (GD18XSH04).

Acknowledgements

This research has been supported by Key-Area Research and Development Program of Guangdong Province, China (2020B0202010002), the National Natural Science Foundation of China (71961137003; 41871148).

References

Aleta, A., Martin-Corral, D., y Piontti, A. P., Ajelli, M., Litvinova, M., Chinazzi, M., … Moreno, Y. (2020). Modelling the impact of testing, contact tracing and household quarantine on second waves of COVID-19. *Nature Human Behaviour, 4*(9), 964–971.

Anderson, R. M., Heesterbeek, H., Klinkenberg, D., & Hollingsworth, T. D. (2020). How will country-based mitigation measures influence the course of the COVID-19 epidemic? *The Lancet, 395*(10228), 931–934.

Buckee, C. O., Balsari, S., Chan, J., Crosas, M., Dominici, F., Gasser, U., … Schroeder, A. (2020). Aggregated mobility data could help fight COVID-19. *Science, 368*, 145–146.

Budd, J., Miller, B. S., Manning, E. M., Lampos, V., Zhuang, M., Edelstein, M., … McKendry, R. A. (2020). Digital technologies in the public-health response to COVID-19. *Nature Medicine, 26*(8), 1183–1192.

Calvo, R. A., Deterding, S., & Ryan, R. M. (2020). Health surveillance during covid-19 pandemic. *British Medical Journal, 369*, m1373.

Chai, Y. (2013). Space–time behavior research in China: Recent development and future prospect: Space–time integration in geography and GIScience. *Annals of the Association of American Geographers, 103*(5), 1093–1099.

Chen, X., Huang, Y., Li, J., Wang, S., & Pei, T. (2020). Clustering characteristics of COVID-19 cases and influencing factors in Chongqing Municipality. *Progress in Geography, 39*(11), 1798–1808.

Chen, W., Liu, L., & Liang, Y. (2016). Retail center recognition and spatial aggregating feature analysis of retail formats in Guangzhou based on POI data. *Geographical Research, 35*(4), 703–716.

Chen, Y., Wang, A., Yi, B., Ding, K., Wang, H., Shi, H., … Xu, G. (2020). The epidemiological characteristics of infection in close contact of COVID-19 in Ningbo city. *Chinese Journal of Epidemiology, 41*(5), 668–672.

China Data Lab. (2020). Harvard dataverse. https://dataverse.harvard.edu/dataverse/data_ncov.

Chinanews. (2021). https://www.chinanews.com/sh/2021/01-10/9383363.shtml. (Accessed 10 January 2021).

Chinazzi, M., et al. (2020). The effect of travel restrictions on the spread of the 2019 novel coronavirus (COVID-19) outbreak. *Science, 368*, 395–400.

Dlamini, W. M., Dlamini, S. N., Mabaso, S. D., & Simelane, S. P. (2020). Spatial risk assessment of an emerging pandemic under data scarcity: A case of COVID-19 in Eswatini. *Applied Geography, 125*, 102358.

Duffus, L. N., Alfa, A. S., & Soliman, A. H. (1987). The reliability of using the gravity model for forecasting trip distribution. *Transportation, 14*(3), 175–192.

Huang, B., Wang, J., Cai, J., Yao, S., Chan, P. K. S., Tam, T. H. W., … Lai, S. (2021). Integrated vaccination and physical distancing interventions to prevent future COVID-19 waves in Chinese cities. *Nature Human Behaviour, 5*(6), 695–705.

Hu, T., Guan, W. W., Zhu, X., Shao, Y., Liu, L., Du, J., … Bao, S. (2020). Building an open resources repository for COVID-19 research. *Data and Information Management, 4*(3), 130–147.

Ienca, M., & Vayena, E. (2020). On the responsible use of digital data to tackle the COVID-19 pandemic. *Nature Medicine, 26*(4), 463–464.

Jia, J. S., Lu, X., Yuan, Y., Xu, G., Jia, J., & Christakis, N. A. (2020). Population flow drives spatio-temporal distribution of COVID-19 in China. *Nature, 582*(7812), 389–394.

Jiang, L. (2012). Study on Guangzhou's employment subcentres and polycentricity. *International Journal of Economics and Management Engineering, 6*(11), 3306–3312.

Kraemer, M. U. G., et al. (2020). The effect of human mobility and control measures on the COVID-19 epidemic in China. *Science, 368*, 493–497.

Kretzschmar, M. E., Rozhnova, G., Bootsma, M. C., van Boven, M., van de Wijgert, J. H., & Bonten, M. J. (2020). Impact of delays on effectiveness of contact tracing strategies for COVID-19: A modelling study. *The Lancet Public Health, 5*(8), e452–e459.

Lai, S., Bogoch, I. I., Ruktanonchai, N. W., Watts, A., Lu, X., Yang, W., … Tatem, A. J. (2020). *Assessing spread risk of Wuhan novel coronavirus within and beyond China, January-April 2020: A travel network-based modelling study*. MedRxiv.

Liu, T., & Chai, Y. (2015). Daily life circle reconstruction: A scheme for sustainable development in urban China. *Habitat International, 50*, 250–260.

Liu, T., Hu, J., Kang, M., Lin, L., Zhong, H., Xiao, J., He, G., Song, T., Huang, Q., & Rong, Z. (2020). Transmission dynamics of 2019 novel coronavirus (2019-nCoV). Available at: SSRN: https://ssrn.com/abstract=3526307.

Li, Q., Guan, X., Wu, P., Wang, X., Zhou, L., Tong, Y., Ren, R., Leung, K. S., Lau, E. H., & Wong, J. Y. (2020). early transmission dynamics in Wuhan, China, of novel coronavirus–infected pneumonia. *New England Journal of Medicine, 382*, 1199–1207. https://doi.org/10.1056/NEJMoa2001316

Lu, J., Zhou, S., Yuan, Q., & Liu, L. (2019). The spatial differentiation of relationship between travel distance and housing rent: Exploring bid-rent mode in polycentric cities. *Shanghai City Planning, 3*, 1–9 (in chineses).

McKenzie, G., & Adams, B. (2020). A country comparison of place-based activity response to COVID-19 policies. *Applied Geography, 125*, 102363.

Mossong, J., Hens, N., Jit, M., Beutels, P., Auranen, K., Mikolajczyk, R., … Edmunds, W. J. (2008). Social contacts and mixing patterns relevant to the spread of infectious diseases. *PLoS Medicine, 5*(3), e74.

Oliver, N., Lepri, B., Sterly, H., Lambiotte, R., Deletaille, S., De Nadai, M., … Vinck, P. (2020). Mobile phone data for informing public health actions across the COVID-19 pandemic life cycle. *Science Advances, 6*, Article eabc0764.

Parker, M. J., Fraser, C., Abeler-Dörner, L., & Bonsall, D. (2020). Ethics of instantaneous contact tracing using mobile phone apps in the control of the COVID-19 pandemic. *Journal of Medical Ethics, 46*(7), 427–431.

Read, J. M., Bridgen, J. R. E., Cummings, D. A. T., Ho, A., & Jewell, C. P. (2020). Novel coronavirus 2019-nCoV: Early estimation of epidemiological parameters and epidemic predictions. *medRxiv*, 2020, 10.23.20018549.

Sanche, S., Lin, Y. T., Xu, C., Romero-Severson, E., Hengartner, N., & Ke, R. (2020). High contagiousness and rapid spread of severe acute respiratory syndrome coronavirus 2. *Emerging Infectious Disease journal, 26*(7), 1470.

Shen, Y., Chai, Y., & Kwan, M. P. (2015). Space–time fixity and flexibility of daily activities and the built environment: A case study of different types of communities in Beijing suburbs. *Journal of Transport Geography, 47*, 90–99.

Shen, M., Peng, Z., Xiao, Y., & Zhang, L. (2020). Modeling the epidemic trend of the 2019 novel coronavirus outbreak in China. *The Innovation, 1*(3), 100048.

Shi, Z., & Zhou, S. (2020). Jobs-housing relationship in different industries and ites impact on traffic demand on road networks : A case study in Guangzhou. *City Planning Review, 44*(2), 87–94. in chinese.

Song, G., Xiao, L., Zhou, S., Long, D., Zhou, S., & Liu, K. (2017). Impact of residents' routine activities on the spatial-temporal pattern of theft from person. *Acta Geographica Sinica, 72*, 356–367.

Tang, B., Wang, X., Li, Q., Bragazzi, N. L., Tang, S., Xiao, Y., & Wu, J. (2020). Estimation of the transmission risk of the 2019-nCoV and its implication for public health interventions. *Journal of Clinical Medicine, 9*(2), 462.

Tian, H., Liu, Y., Li, Y., Wu, C. H., Chen, B., Kraemer, M. U., & Dye, C. (2020). An investigation of transmission control measures during the first 50 days of the COVID-19 epidemic in China. *Science, 368*(6491), 638–642.

Wang, J., Li, G., Wang, J., Qiang, J., & Zhu, D. (2020). Spatiotemporal evolution and risk profiling of the COVID-19 epidemic in shaanxi province. *Tropical Geography, 40*(3), 432–445.

Wei, Y., Wang, J., Song, W., Xiu, C., Ma, L., & Pei, T. (2021). Spread of COVID-19 in China: Analysis from a city-based epidemic and mobility model. *Cities, 110*, 103010.

Wu, J. T., Leung, K., & Leung, G. M. (2020). Nowcasting and forecasting the potential domestic and international spread of the 2019-nCoV outbreak originating in Wuhan, China: A modelling study. *The Lancet, 395*(10225), 689–697.

Wu, J. T., Leung, K., & Leung, G. M. (2020). Nowcasting and forecasting the potential domestic and international spread of the 2019-nCoV outbreak originating in Wuhan, China: A modelling study. *The Lancet, 395*(10225), 689–697.

Yechezkel, M., Weiss, A., Rejwan, I., Shahmoon, E., Gal, S. B., & Yamin, D. (2020). *Human mobility and poverty as key factors in strategies against COVID-19. medRxiv*.

Yin, L., Zhang, H., Li, Y., Liu, K., Chen, T., Luo, W., … Mei, S. (2021). A data driven agent-based model that recommends non-pharmaceutical interventions to suppress Coronavirus disease 2019 resurgence in megacities. *Journal of the Royal Society Interface, 18*(181), 20210112. https://doi.org/10.1098/rsif.2021.0112.

Zhang, P., Zhou, J., & Zhang, T. (2017). Quantifying and visualizing jobs-housing balance with big data: A case study of Shanghai. *Cities, 66*, 10–22.

Zheng, Z., Zhou, S., & Deng, X. (2021). Exploring both home-based and work-based jobs-housing balance by distance decay effect. *Journal of Transport Geography, 93*, 103043.

Zhou, S., & Yan, X. (2005). The spatial structure of residential and industrial land use in Guangzhou. *Scientia Geographica Sinica, 25*(6), 664–670.

Zhou, S., & Deng, L. (2010). Spatio-temporal pattern of residents' daily activities based on T-GIS: A case study in Guangzhou, China. *Acta Geographica Sinica, 65*(12), 1454–1463.

Zhou, C., Su, F., Pei, T., Zhang, A., Du, Y., Luo, B., … Xiao, H. (2020). COVID-19: Challenges to GIS with big data. *Geography and sustainability, 1*(1), 77–87.

Zhou, S, Zhou, S, Zheng, Z, & Lu, J (2021). Optimizing spatial allocation of COVID-19 vaccine by agent-based spatiotemporal simulations. *GeoHealth, 5*(6), Article e2021GH000427.